Chemistry & Biology, Vol. 9, 163–169, February, 2002, ©2002 Elsevier Science Ltd. All rights reserved. PII S1074-5521(02)00102-3

Cell Aggregation by Scaffolded Receptor Clusters

Jason E. Gestwicki,[2] Laura E. Strong,[1,4] Christopher W. Cairo,[1] Frederick J. Boehm,[1] and Laura L. Kiessling,[1,2,3]
[1]Department of Chemistry
[2]Department of Biochemistry
University of Wisconsin-Madison
Madison, Wisconsin 53706

Summary

The aggregation of cells by lectins or antibodies is important for biotechnological and therapeutic applications. One strategy to augment the avidity and aggregating properties of these mediators is to maximize the number of their ligand binding sites. The valency of lectins and antibodies, however, is limited by their quaternary structures. To overcome this limitation, we explored the use of polymers generated by ring-opening metathesis polymerization (ROMP) as scaffolds to noncovalently assemble multiple copies of a lectin, the tetravalent protein concanavalin A (Con A). We demonstrate that complexes between Con A and multivalent scaffolds aggregate cells of a T cell leukemia line (Jurkat) more effectively than Con A alone. We anticipate that synthetic scaffolds will offer a new means of facilitating processes that rely on cell aggregation, such as pathogen clearance and immune recognition.

Introduction

Many proteins, including lectins and antibodies, possess multiple ligand binding sites. These proteins can mediate cell aggregation by binding to cell surface ligands on apposing cells. Cell aggregation is a key event that has been exploited for the development of diagnostics for pathogen detection [1], therapeutics [2–5], blood-typing tests [6], and other biotechnological applications [7–9]. One of the most exciting applications of this technology has been the targeted aggregation of pathogenic species. Aggregation of pathogenic entities (e.g., bacteria [5] or phage particles [10]) can lead to the clearance of the resulting aggregates [11] and protection from infection [12, 13]. The propensity of a multivalent protein to mediate cell aggregation is determined by how avidly it binds to the cell surface. One effective way to increase the avidity of these interactions is to increase the number of cell surface binding pockets [14–16]. Efforts aimed at this objective have focused on generating novel multimers of antibody scFv fragments [17, 18] or favoring oligomer formation for lectins [19–21].

Lectins are a large class of saccharide binding proteins, many of which are homo-oligomers assembled from two to four copies of identical subunits [22, 23]. Lectins aggregate cells when they crosslink glycoproteins or glycolipids on adjacent cell surfaces. Aggregation can be modulated by altering the number of active monomers within the lectin oligomer. For example, the ability of the mannose binding plant lectin concanavalin A (Con A) to aggregate red blood cells is greatly decreased when the lectin is forced from the tetrameric into the dimeric form by succinylation [20]. Increasing the valency of a lectin would be expected to enhance its ability to promote cell aggregation. Methods for generating soluble lectin complexes with higher-order valencies, however, have not been described. We sought to develop a strategy for the formation of lectin assemblies with valencies beyond those accessible to natural lectins. We envisioned that the resulting complexes would possess enhanced cell aggregation properties.

To augment cell avidity, we set out to assemble a natural lectin on a synthetic scaffold. It has been shown that low-molecular-weight synthetic ligands displaying a few carbohydrate residues can interact with multiple copies of lectins [21, 24–27]. For example, divalent or trivalent displays of mannose can assemble soluble clusters of Con A tetramers [28, 29]. We envisioned that extended polymeric displays of mannose would also possess this ability; thus, these carbohydrate-bearing ligands could be used as templates to create macromolecular assemblies containing multiple lectins. We have previously synthesized polymers displaying mannose by ring-opening metathesis polymerization (ROMP) [30]. ROMP allows the generation of linear polymer chains of distinct valencies [31] bearing pendant residues competent for interaction with cell surfaces [32–34] or soluble receptors, including the lectin Con A [30, 35–38]. Based on the activity of these materials in assays with Con A, we hypothesized that multiple Con A tetramers could assemble on these polymers by interaction of the lectins with the pendant mannose residues [38]. We predicted that the lectin-polymer complex would possess unoccupied mannose binding sites for interaction with cell surface ligands [28].

Materials synthesized by ROMP are well-suited to these studies because their average length can be controlled. The ability to control this feature of the polymers is due to the relatively fast rate of initiation compared to that of propagation. The ratio of monomer to catalyst in these reactions determines the average chain length of the resultant polymer [39–41]. Thus, we could explore the effect that the number of mannose residues has on the number of Con A tetramers that are assembled. We found that polymer valency determines the average number of Con A tetramers that assemble on the oligomeric scaffold. Moreover, the resulting Con A-polymer complexes are highly effective agents for aggregating cells.

Results and Discussion

Multivalent ROMP-Derived Scaffolds Can Induce Con A Precipitation

A scaffold must bind multiple Con A tetramers to generate higher-order lectin clusters. We examined the ability

[3]Correspondence: kiessling@chem.wisc.edu
[4]Present address: Quintessence Biosciences, University Research Park, 505 South Rosa Road, Madison, Wisconsin 53719.

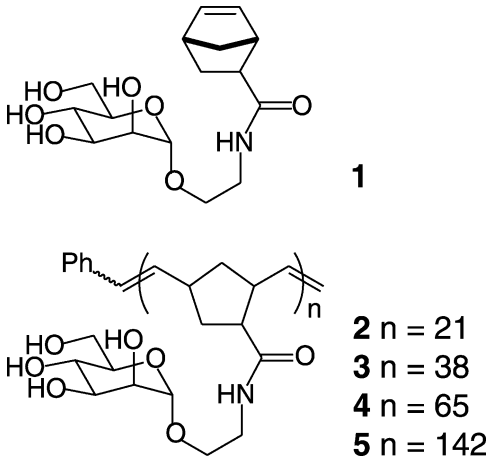

Figure 1. Chemical Structures of Mannose-Bearing Compounds
The average valency (n) was calculated by using ^{1}H NMR integration.

of ROMP-derived oligomers (Figure 1) to assemble multiple Con A tetramers by using quantitative precipitation (Figure 2A). The precipitation of Con A depends on the clustering of Con A tetramers, and this endpoint has been used to determine the stoichiometry of insoluble Con A-ligand complexes [42]. When **1–5** were introduced to Con A, monomeric compound **1** was unable to induce precipitation, as expected. Multivalent ligands **2–5**, however, caused concentration-dependent precipitation of Con A. The concentration of the higher-valency materials **3–5** that was required to induce precipitation was lower than that required for the shorter oligomer **2**. The concentration of **2** required to induce maximum precipitation was 18 μM (calculated by the concentration of polymer, see Experimental Procedures), approximately one half of the concentration of Con A tetramers in solution. This indicates that the stoichiometry of Con A tetramers per scaffold in these precipitates is approximately 2:1 [42]. The concentrations of **3**, **4**, and **5** that were required to induce maximum precipitation were substantially lower (6 μM, 9 μM, and 5 μM, respectively). These correspond to stoichiometries of approximately 4–6 Con A tetramers per scaffold.

To further examine the effects of valency on Con A assembly, we conducted additional precipitation experiments with dimeric succinylated Con A. Compared to the precipitation of tetrameric Con A, the precipitation of succinylated Con A is less efficient [42]. Only the highest valency compounds **4** and **5** were able to precipitate succinylated Con A (Figure 2B). The concentration of **4** that was required for maximum precipitation of succinylated Con A was 10 μM, one fourth the concentration of succinylated Con A dimers present in these assays (44 μM), indicating a 4:1 (receptor:scaffold) stoichiometry in the precipitate. The concentration of **5** that was required for maximum precipitation was 5 μM, indicating a stoichiometry of approximately 9 receptors per scaffold. These results suggest that the number of mannose units displayed by the scaffold is a key determinant in the formation of insoluble protein-scaffold complexes.

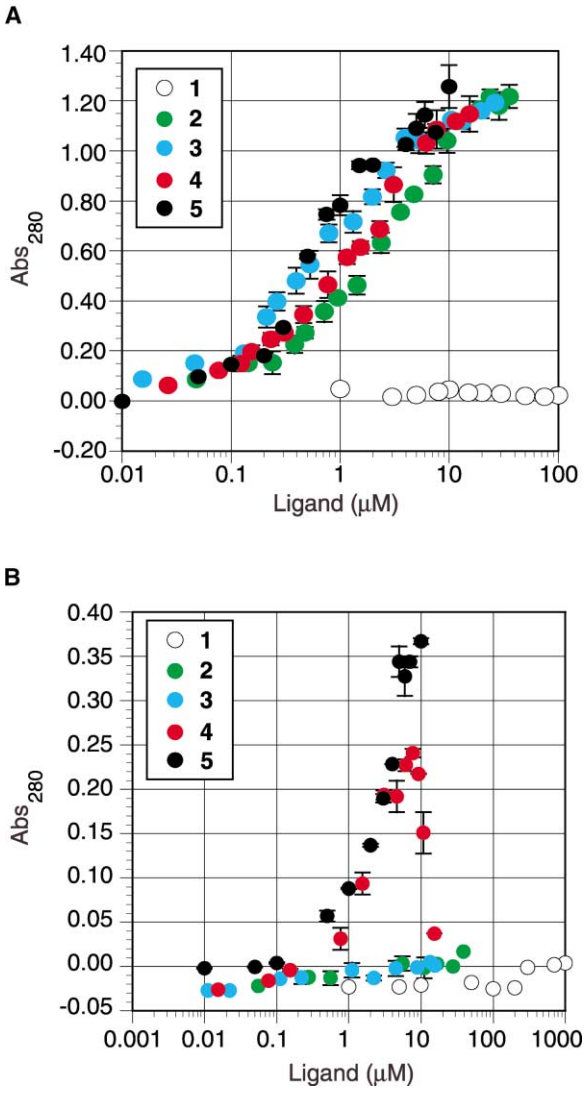

Figure 2. Quantitative Precipitation of Con A

(A) Compounds **1–5** were used to precipitate tetrameric Con A.

(B) Compounds **1–5** were used to precipitate succinylated Con A. Ligand concentration in these graphs is plotted as a function of polymer concentration, which is determined by using the degree of polymerization (dp) to calculate average molecular weight. Results are the average of three independent experiments, and error bars represent single standard deviations. Some error bars are smaller than the symbols.

Multivalent ROMP-Derived Scaffolds Form Soluble Aggregates of Con A in Solution

The quantitative precipitation results demonstrated that Con A clusters can form in the presence of multivalent polymers. These experiments examined insoluble clusters, however, and we sought to characterize the formation of clusters in solution. The assembly of Con A on mannose scaffolds in solution can be monitored by FRET [28]. Con A can be labeled with either fluorescein to generate a donor for FRET or tetramethylrhodamine (TMR) [43, 44] to generate an acceptor. When these derivatives are within approximately 80 Å of each other, the fluorescein emission intensity is quenched. Although

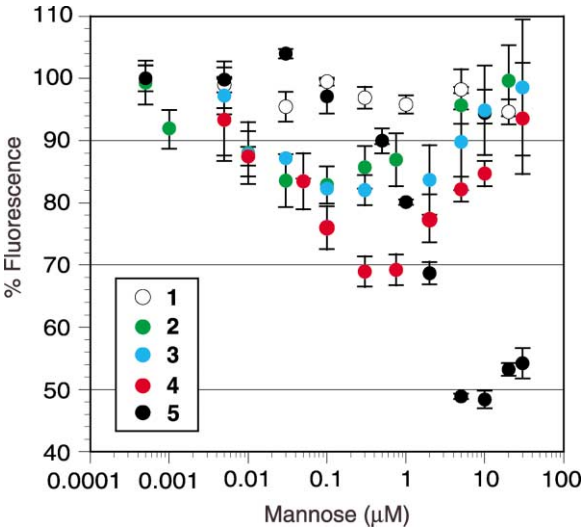

Figure 3. FRET Experiments

Compounds **1–5** were each added to a mixture of fluorescein- and TMR-Con A as discussed in the Experimental Procedures. The emission intensity of fluorescein is plotted as the percent of the fluorescence of an untreated sample. Concentrations on the *x* axis refer to the concentration of mannose residues. Results are the average of three to five independent experiments, and error bars represent single standard deviations.

the formation of insoluble aggregates also could influence the FRET signal, these do not form at the low concentrations of fluorescent protein needed for FRET experiments. Thus, changes in fluorescence intensity probably report on the formation of soluble clusters.

Compounds **1–5** were each added to a solution containing fluorescein- and TMR-labeled Con A. We monitored the emission intensity of fluorescein at 520 nm to ascertain whether these scaffolds promote the formation of soluble Con A clusters. Con A was clustered in the presence of multivalent polymers **2–5** but not monomeric compound **1** (Figure 3). The maximum quenching induced by **4** and **5** was greater (30% and 50% respectively) than that caused by the lower-valent compounds **2** and **3** (18%). The scaffolds **1–5** were not fluorescent at 520 nm (data not shown). This result provides further evidence that the extent of Con A clustering depends on scaffold valency.

The fluorescence quenching was dependent not only on the valency of the multivalent mannose derivative but also on its concentration. Interestingly, the efficiency of quenching first increased as scaffold concentration increased and then decreased as the concentration was increased further. The absence of quenching at high multivalent ligand concentrations suggests that Con A clusters are disfavored at these concentrations. As stated above, we could not detect the formation of insoluble clusters, and the polymer displays are not fluorescent. Thus, the most likely mechanism for the increase is that mannose binding site saturation is occurring. When polymer concentrations are high, each mannose binding site on Con A can be occupied by an individual polymer, thereby precluding the clustering of multiple lectins. Thus, complexes containing multiple Con A tetramers could be assembled readily on **2–5** when intermediate multivalent scaffold concentrations (e.g., mannose residue concentrations of 0.5–5 μM) were used, but they were less likely to form when the concentration of the scaffold was either lower (< 0.1 μM mannose

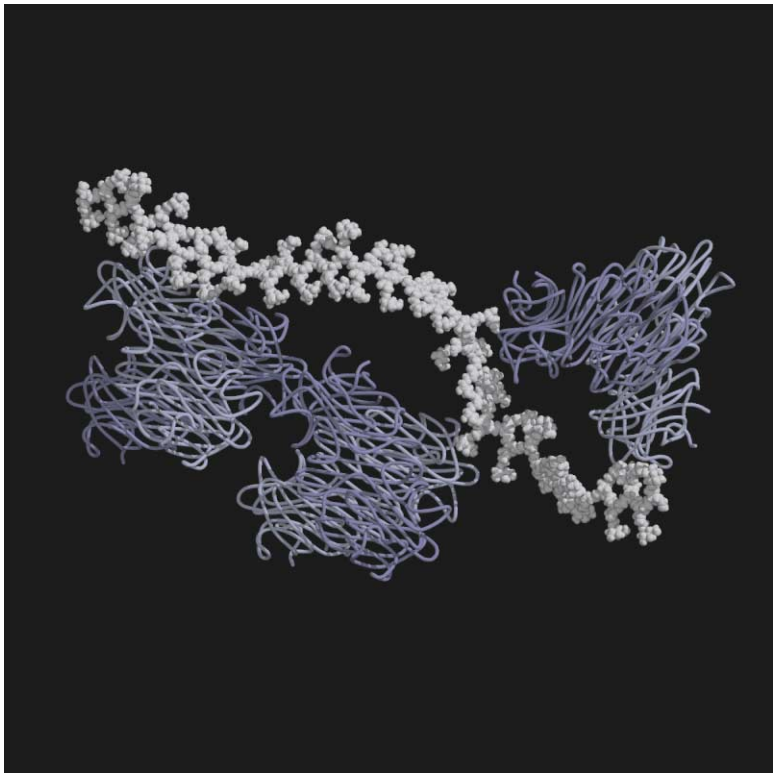

Figure 4. Proposed Complex between Con A and a Multivalent ROMP-Derived Scaffold

A polymer of 50 monomer units was modeled in MacroModel 6.5, as discussed in the Experimental Procedures. A complex was assembled between this polymer and Con A tetramers. The structure of Con A was previously determined by X-ray crystallography [50]. The stoichiometry was chosen on the basis of results from transmission electron microscopy experiments [38] and the quantitative precipitation and FRET results presented here.

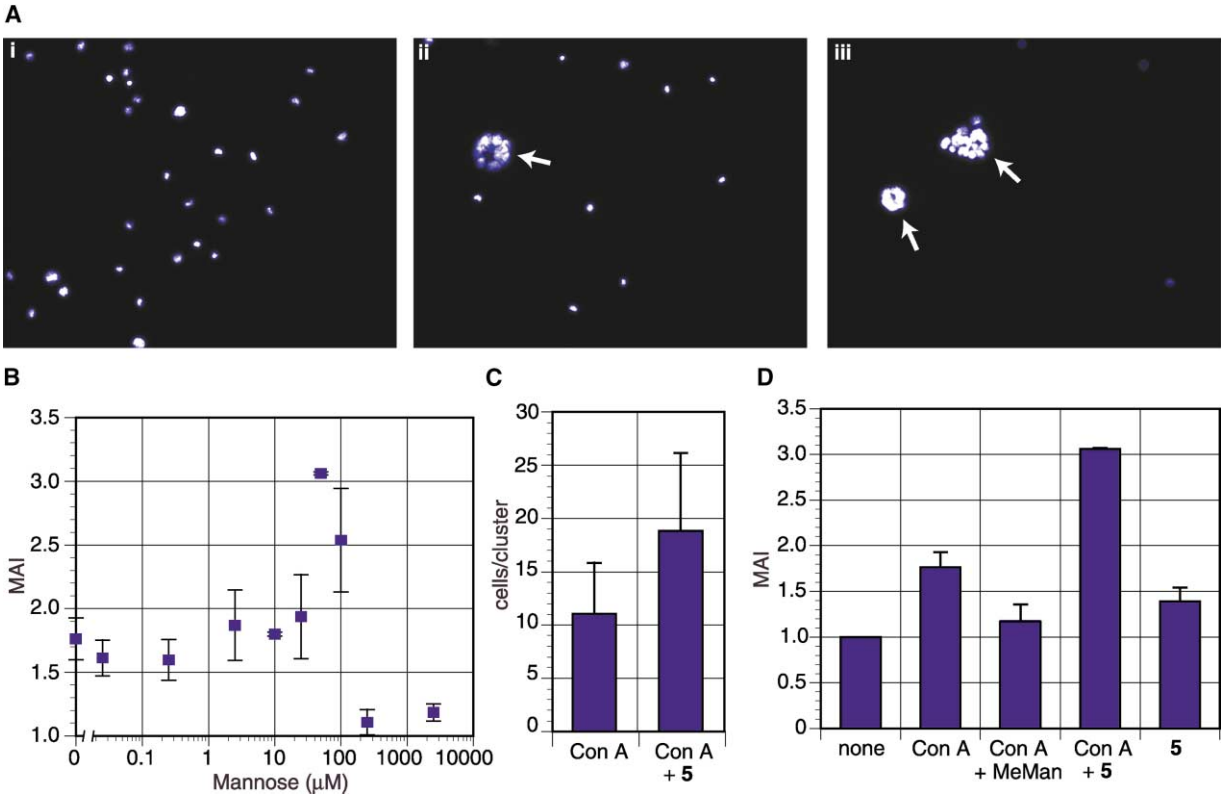

Figure 5. Aggregation of Jurkat Cells by Con A and Scaffolded Con A

(A) Selected microscopy fields show the results of experiments in which cells were labeled with a fluorescent dye and treated with buffer (i), Con A (75 μg/mlL, ii), or Con A with 50 μM **5** (iii). Jurkat cells were fixed with 2% paraformaldehyde to prevent activation of the cells by Con A. Con A concentrations are calculated based on the tetrameric form, and ligand concentrations are reported as mannose residue concentrations. Arrows point to aggregates. All fields are at 200× magnification.

(B) Quantitation of microscopy fields as described in the Experimental Procedures. A solution of **5** and Con A was added to Jurkat cells, and the macroscopic aggregation index (MAI) was determined as previously described [53]. Results are the average of 2–4 independent experiments, and error bars represent single standard deviations.

(C) The average number of cells included in clusters was determined with image analysis, as described in the Experimental Procedures. Clustering was mediated by either 75 μg/ml Con A alone or Con A with **5** (50 μM mannose residues). Error bars represent the standard deviation.

(D) Jurkat cells were aggregated with Con A at 75 μg/ml, and the MAI was determined by microscopy. The addition of 100 mM methyl α-D-mannopyranoside (MeMan) disrupted Con A-induced aggregate formation. Complexes of Con A and **5** were formed from 75 μg/ml Con A and **5** (50 μM mannose residues). Compound **5** alone possessed little or no ability to aggregate cells, even at high concentrations (2.5 mM mannose residues).

residues) or higher (> 50 μM mannose residues). These data reveal that cluster formation can be controlled by scaffold valency and concentration.

Scaffolded Con A Enhances Aggregation of Leukemia Cells

We hypothesized that, under conditions that favor macromolecular complexation, lectins assembled on polymer scaffolds would possess unoccupied saccharide binding sites (Figure 4). These sites would be poised to interact avidly with cell surface glycoproteins, and complexation of adjacent cell surfaces would result in cell aggregation. To test this hypothesis, we studied the ability of Con A-scaffold complexes to aggregate cells of the Jurkat human T cell leukemia line.

When Con A was added to fluorescently labeled Jurkat cells, cell aggregation occurred (Figure 5). Aggregates were visualized by fluorescence microscopy, and the amount of aggregation was quantitated by determination of the macroscopic aggregation index (MAI; see Experimental Procedures). Upon the addition of a premixed solution of **5** (50 μM mannose residues) and Con A (75 μg/ml), an enhancement of cell aggregation of approximately 60% over Con A alone was observed (Figure 5B). This increase in MAI was not due to the disruption of large aggregates into smaller clusters of cells; the aggregates that formed in the presence of the mixture of Con A and **5** were of similar or greater size than those formed by Con A alone (Figure 5C). Without Con A, **5** was a poor aggregating agent (Figure 5D), indicating that the combination of **5** and Con A was necessary for the enhanced aggregation of cells. Cell aggregation was sensitive to the concentration of **5**. High concentrations of **5** disrupted aggregation, presumably by saturating saccharide binding sites on Con A. This result is consistent with that expected from the

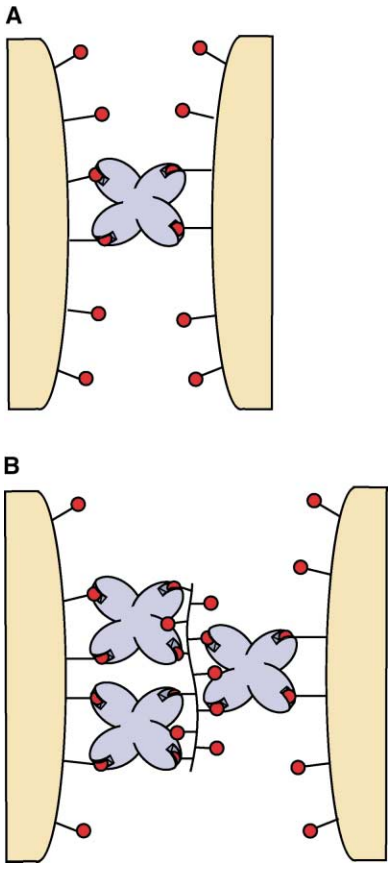

Figure 6. Models for the Aggregation of Cells by Con A

(A) Two hypothetical cell surfaces bearing multiple mannose-terminated glycans (red circles) can be aggregated by tetravalent Con A.

(B) The observed enhancements in cell aggregation in the presence of multivalent ligands probably arise from the increased avidity of the Con A-scaffold complex for the cell surface. It is highly unlikely that the Con A-scaffold complexes span more than two cell surfaces simultaneously; the total length of the complex [38] is approximately 20 nm, and the average size of a Jurkat cell is between 5,000 and 10,000 nm.

lack of FRET at high multivalent ligand concentrations. We postulate that the enhanced aggregation of Jurkat cells by scaffolded Con A is due to the increased avidity of the complexes for cell surface glycans and that this increase occurs as a result of an increase in available binding sites (Figure 6).

Our results demonstrate a new use for multivalent compounds. Multivalent ligands have been used as highly effective inhibitors of biological recognition events [15, 45, 46]. Their ability to cluster proteins has also been exploited to provide ligands that act as effectors (rather than inhibitors) of a response [47, 48]. We demonstrate here that, in addition to these previously recognized uses, multivalent compounds also can serve as templates for the formation of macromolecular assemblies. In this capacity, multivalent ligands can serve as vehicles for the facile aggregation of cells.

The multivalent mannose derivatives we describe here assemble multiple Con A tetramers through noncovalent protein-saccharide interactions. The use of synthetic multivalent materials for the presentation of multiple copies of a protein may also be accomplished by covalent attachment. We expect that these modes of protein presentation will find application in the development of diagnostic and therapeutic agents.

Significance

The binding of a multivalent receptor to multiple cell surface ligands can promote cell and viral particle aggregation. The strength and stability of these interactions are dependent on the number of unoccupied sites available for receptor binding to the cell surface. Here we have shown that ROMP-derived materials of sufficient valency can act as scaffolds for the assembly of multiple Con A tetramers; the resulting clusters are highly effective mediators of cell aggregation. The ability of these polymers to assemble clusters depends on their valency and concentration; thus, the activity of the scaffold is tunable. These results offer new avenues for sensitive diagnostic agents and the synthesis of materials that facilitate the clearance of pathogens.

Experimental Procedures

Synthesis of Multivalent Ligands

The syntheses and Con A binding properties of compounds **1–4** have been reported [30]. Compound **5** was synthesized by an analogous route. The average valency (n) is based on the calculated degree of polymerization (dp) for each compound as determined by ^{1}H NMR spectroscopy.

Quantitative Precipitation

Quantitative precipitation experiments and their analyses were carried out by a method modified from that previously described by Khan et al. [42]. In brief, Con A (Vector Laboratories, Burlingame, CA) and scaffold were dissolved in precipitation buffer (0.1 M Tris-HCl [pH 7.5], 90 μM NaCl, 1 mM $CaCl_2$, 1 mM $MnCl_2$), vortexed briefly to mix, and then incubated for 5 hr at room temperature (or 2 days at 4°C for succinylated Con A). The final concentration of Con A tetramers was 30 μM (if one assumes Con A tetramers to have a molecular mass of 104,000 Da), and that of succinylated Con A dimers was 44 μM (if one assumes that dimers have a mass of 52,000 Da). The concentrations of mannose-bearing polymers are estimated based on the dp for each polymer. In all other experiments, the concentrations are based on total mannose concentration (or mannose residue).

The white precipitates that formed after the incubation period were pelleted by centrifugation at 5000 × g for 2 min. Supernatants were removed by pipet, and pellets were gently washed twice with ice-cold precipitation buffer. Pellets were then resuspended in 600 μl 100 mM methyl α-D-mannopyranoside (100 μl for succinylated Con A) and were completely dissolved after a 10 min incubation at room temperature. Protein content was determined by measurement of the absorbance at 280 nm on a Varian Cary 50 Bio UV-vis spectrometer and a 100 μl volume quartz cuvette. Measurements are the average of three independent experiments.

Fluorescence Resonance Energy Transfer

Fluorescein-Con A (Vector Laboratories, Burlingame, CA) and TMR-Con A (Sigma, St. Louis, MO) dissolved in phosphate-buffered saline (PBS) (pH 7.2) were mixed to afford final concentrations of 4 μg/ml and 0.4 μg/ml, respectively. Mannose-displaying scaffold was added in PBS to the final concentration indicated (Figure 3), with a final volume of 200 μl. The reported concentration was determined based on the total mannose residue concentration. The resulting mixtures were vortexed briefly and then incubated at room temperature for at least 15 min. The fluorescence emission intensity was

determined on a Hitachi F-4500 fluorospectrophotometer by the use of a 200 μl volume quartz cuvette, an excitation wavelength of 492 nm, emission wavelength of 515 nm, and 10 nm slit widths. Emission intensities are the average of 3–5 independent experiments, with three scans performed during each experiment. Compounds **1–5** had negligible fluorescence at 515 nm (our unpublished data). No significant difference in fluorescein intensity was observed before or after centrifugation (at 9300 × g for 5 min) of freshly prepared samples of fluorescent Con A and polyvalent scaffold. We conclude that the scaffolded clusters of fluorescent Con A that formed at low concentrations were soluble.

Molecular Modeling

To aid in the assembly of a model of macromolecular scaffold-Con A complexes, we built isotactic polymers based on structures **2–5** with Macromodel 6.5 (Schrodinger Inc., Portland, OR). We minimized these structures first by using distance constraints to induce an extended conformation, then again without constraints. All calculations used the AMBER* force field in vacuo [49]. Average polymer lengths were calculated from these conformations.

The dimer of Con A tetramers (see Figure 5) was generated with the symmetry operator of the crystal (1CVN, $P_{1\,21\,1}$) [50] and represents one favorable tetramer-tetramer interaction. The Con A tetramers were then assembled onto an extended polymer structure in a random conformation with Macromodel 6.5. The stoichiometry of the complex was designated by the determined polymer length in addition to both the results from the FRET, the quantitative precipitation experiments presented above, and results from previous studies [38]. The figure was generated with Molscript version 2.1.2 and Raster 3D version 2.3 [51, 52].

Jurkat Cell Aggregation

Jurkat cells were cultured and maintained as described [34]. Cells (approximately 1×10^7/ml) were washed three times in cold Ca^{2+}-enriched HEPES-buffered saline (pH 7.2) (HBS-Ca^{2+}; HBS + 1 mM $CaCl_2$) and then treated with Hoescht 33342 (100 μg/ml) for 30 min at 30°C. Cells were washed twice with cold HBS-Ca^{2+} and then fixed for 30 min at 4°C with 2% paraformaldehyde in HEPES buffer (pH 7.4). Fixed cells were washed twice and then treated in 6 μl final volume with premixed solutions of Con A and scaffold. A 2× solution of Con A and scaffold was prepared in HBS-Ca^{2+} and then incubated at 22°C for 15 min before being added to cells. Cells, Con A solutions, and 100 μg/ml DNase (for preventing cell aggregation by nucleic acid) were added directly to a clean glass slide, and the mixture was incubated at 4°C for 30 min. Visualization was performed at 200× magnification on a Zeiss Axioscope outfitted with the appropriate filter set. Approximately 200–350 cells were counted from a total of 10 random fields on each day. The total number of particles was used for determining the macroscopic aggregation index (MAI) [53]. Briefly explained, MAI is determined by dividing the number of particles from 10 random fields of a control sample by the number from a treated sample. Aggregate formation results in fewer particles and a larger MAI value. The average number of cells included in the aggregates was with NIH Image 1.6.2. The fluorescence intensity of individual cells and clusters of cells was measured with this software, and the fluorescence intensity of the clusters was divided by the average individual cell's intensity. Compounds **1–5** were not able to cause cell aggregation alone (data not shown for **1–4**). Images were captured in IPlab Spectra 3.2 and prepared in Adobe PhotoShop 5.0.

Acknowledgments

We acknowledge Drs. M.C. Schuster and D.A. Mann for helpful conversations and Prof. S. Bednarek (University of Wisconsin-Madison) for the generous use of fluorescence microscopy equipment. This research was supported by the National Institutes of Health (GM55984). J.E.G. thanks the Biotechnology Training Program for a predoctoral fellowship (GM08349). L.E.S. was supported by a National Institutes of Health predoctoral fellowship (GM18750). F.J.B. thanks the Hilldale Undergraduate Research Fellowship Program for support.

Received: July 23, 2001
Revised: October 1, 2001
Accepted: October 4, 2001

References

1. Kemp, B.E., Rylatt, D.B., Bundesen, P.G., Doherty, R.R., McPhee, D.A., Stapleton, D., Cottis, L.E., Wilson, K., John, M.A., Khan, J.M., et al. (1988). Autologous red cell agglutination assay for HIV-1 antibodies: simplified test with whole blood. Science *241*, 1352–1354.
2. Kawauchi, H., Hosono, M., Takayanagi, Y., and Nitta, K. (1993). Agglutinins from aquatic insects-tumor cell agglutination activity. Experientia *49*, 358–361.
3. Coloma, M.J., and Morrison, S.L. (1997). Design and production of novel tetravalent bispecific antibodies. Nat. Biotechnol. *15*, 159–163.
4. Segal, D.M., Weiner, G.J., and Weiner, L.M. (1999). Bispecific antibodies in cancer therapy. Curr. Opin. Immunol. *11*, 558–562.
5. Taylor, R.P., Nardin, A., and Sutherland, W.M. (1997). Clearance of blood-borne pathogens mediated through bispecific monoclonal antibodies bound to the primate erythrocyte complement receptor. Cancer Immunol. Immunother. *45*, 152–155.
6. Furata, M., Uchikawa, M., Ueda, Y., Yabe, T., Taima, T., Tsumoto, K., Kojima, S., Juji, T., Kumagai, I., et al. (1998). Construction of mono- and bivalent human single-chain Fv fragments against the D antigen in the Rh blood group: multimerization effect on cell agglutination and application to blood typing. Protein Eng. *11*, 233–241.
7. Singh, R.S., Tiwary, A.K., and Kennedy, J.F. (1999). Lectins: sources, activities, and applications. Crit. Rev. Biotechnol. *19*, 145–178.
8. Matsuya, Y., and Yamane, I. (1985). Cell hybridization and cell agglutination 1. Enhancement of cell hybridization by lectins. J. Cell Sci. *78*, 263–271.
9. Takamatsu, H., Kawajiri, H., Takahashi, Y., Manaf Ali, A., and Yoshimoto, T. (1999). Continuous antibody production by phytohemagglutinin-L-aggregated hybridoma cells. J. Immunol. Methods *223*, 165–170.
10. Taylor, R.P., Martin, E.N., Reinagel, M.L., Nardin, A., Craig, M., Choice, Q., Schlimgen, R., Greenbaum, S., Incardona, N.L., Ochs, H.D., et al. (1997). Bispecific monoclonal antibody complexes facilitate eryhthrocyte binding and liver clearance of a prototype particulate pathogen in a monkey model. J. Immunol. *159*, 4035–4044.
11. Nardin, A., Schlimgen, R., Holers, V.M., and Taylor, R.P. (1999). A prototype pathogen bound ex vivo to human erythrocyte complement receptor 1 via bispecific monoclonal antibody complexes is cleared to the liver in a mouse model. Eur. J. Immunol. *29*, 1581–1586.
12. Lindorfer, M.A., Nardin, A., Foley, P.L., Solga, M.D., Bankovich, A.J., Martin, E.N., Henderson, A.L., Price, C.W., Gyimesi, E., Wozencraft, C.P., Goldberg, J.B., Sutherland, W.M., Taylor, R.P., et al. (2001). Targeting of *Pseudomonas aeruginosa* in the bloodstream with bispecific monoclonal antibodies. J. Immunol. *167*, 2240–2249.
13. Craig, M., Reinagel, M., Martin, E.N., Schlimgen, R., Nardin, A., and Taylor, R.P. (1999). Infusion of bispecific monoclonal antibody complexes into monkeys provides immunologic protection against later challenge with model pathogen. Clin. Immunol. *92*, 170–180.
14. Crothers, D.M., and Metzger, H. (1972). The influence of polyvalency on the binding properties of antibodies. Immunochemistry *9*, 341–357.
15. Mammen, M., Choi, S.-K., and Whitesides, G.M. (1998). Polyvalent interactions in biological systems: implications for design and use of multivalent ligands and inhibitors. Angew. Chem. Int. Ed. Engl. *37*, 2755–2794.
16. Kiessling, L.L., and Pohl, N.L. (1996). Strength in numbers: nonnatural polyvalent carbohydrate derivatives. Chem. Biol. *3*, 71–77.
17. Hudson, P.J., and Kortt, A.A. (1999). High avidity scFv multimers; diabodies and triabodies. J. Immunol. Methods *231*, 177–189.

18. Todorovska, A., Roovers, R.C., Dolezal, O., Kortt, A.A., Hoogenboom, H.R., and Hudson, P.J. (2001). Design and application of diabodies, tribodies, and tetrabodies for cancer targeting. J. Immunol. Methods *248*, 47–66.
19. Torti, M., Ramaschi, G., Sinigaglia, F., and Balduini, C. (1995). Dual mechanism of protein-tyrosine phosphorylation in concanavalin A-stimulated platelets. J. Cell. Biochem. *57*, 30–38.
20. Osawa, T., and Beppu, M. (1987). Cross-linked derivatives of concanavalin A. Methods Enzymol. *150*, 17–28.
21. Sacchettini, J.C., Baum, L.G., and Brewer, C.F. (2001). Multivalent protein-carbohydrate interactions: a new paradigm for supermolecular assembly and signal transduction. Biochemistry *40*, 3009–3015.
22. Weis, W.I., Taylor, M.E., and Drickamer, K. (1998). The C-type lectin superfamily in the immune system. Immunol. Rev. *163*, 19–34.
23. Lis, H., and Sharon, N. (1998). Lectins: carbohydrate-specific proteins that mediate cellular recognition. Chem. Rev. *98*, 637–674.
24. Bezouska, K., Kren, V., Kieburg, C., and Lindhorst, T.K. (1998). GlcNAc-terminated glycodendrimers form defined precipitates with the soluble dimeric receptor of rat natural killer cells, sNKR-P1A. FEBS Lett. *426*, 243–247.
25. Garcia-Lopez, J.J., Hernandez-Mateo, F., Isac-Garcia, J., Kim, J.M., Roy, R., Santoyo-González, F., and Vargas-Berenguel, A. (1999). Synthesis of per-glycosylated β-cyclodextrins having enhanced lectin binding affinity. J. Org. Chem. *64*, 522–531.
26. Kitov, P.I., Sadowska, J.M., Mulvey, G., Armstrong, G.D., Ling, H., Pannu, N.S., Read, R.J., and Bundle, D.R. (2000). Shiga-like toxins are neutralized by tailored multivalent carbohydrate ligands. Nature *403*, 669–672.
27. Lundquist, J.J., Debenham, S.D., and Toone, E.J. (2000). Multivalency effects in protein-carbohydrate interaction: the binding of the Shiga-like toxin 1 binding subunit to multivalent C-linked glycopeptides. J. Org. Chem. *65*, 8245–8250.
28. Burke, S.D., Zhao, Q., Schuster, M.C., and Kiessling, L.L. (2000). Synergistic formation of soluble lectin clusters by a templated multivalent saccharide ligand. J. Am. Chem. Soc. *122*, 4518–4519.
29. Dimick, S.M., Powell, S.C., McMahon, S.A., Moothoo, D.N., Naismith, J.H., and Toone, E.J. (1999). On the meaning of affinity: cluster glycoside effects and concanavalin A. J. Am. Chem. Soc. *121*, 10286–10296.
30. Strong, L.E., and Kiessling, L.L. (1999). A general synthetic route to defined, biologically active multivalent arrays. J. Am. Chem. Soc. *121*, 6193–6196.
31. Kiessling, L.L., and Strong, L.E. (1998). Bioactive polymers. Top. Organomet. Chem. *1*, 199–231.
32. Gestwicki, J.E., Strong, L.E., and Kiessling, L.L. (2000). Tuning chemotactic responses using synthetic multivalent ligands. Chem. Biol. *7*, 583–591.
33. Gordon, E.J., Sanders, W.J., and Kiessling, L.L. (1998). Synthetic ligands point to cell surface strategies. Nature *392*, 30–31.
34. Gordon, E.J., Gestwicki, J.E., Strong, L.E., and Kiessling, L.L. (2000). Synthesis of end-labeled multivalent ligands for exploring cell-surface-receptor-ligand interactions. Chem. Biol. *7*, 9–16.
35. Mortell, K.H., Gingras, M., and Kiessling, L.L. (1994). Synthesis of cell agglutination inhibitors by aqueous ring-opening metathesis polymerization. J. Am. Chem. Soc. *116*, 12053–12054.
36. Mann, D.A., Kanai, M., Maly, D.J., and Kiessling, L.L. (1998). Probing low affinity and multivalent interactions with surface plasmon resonance: ligands for concanavalin A. J. Am. Chem. Soc. *120*, 10575–10582.
37. Kanai, M., Mortell, K.H., and Kiessling, L.L. (1997). Varying the size of multivalent ligands: the dependence of concanavalin A binding on neoglycopolymer length. J. Am. Chem. Soc. *119*, 9931–9932.
38. Gestwicki, J.E., Strong, L.E., and Kiessling, L.L. (2000). Visualization of single multivalent receptor-ligand complexes by transmission electron microscopy. Angew. Chem. Int. Ed. Engl. *39*, 4567–4570.
39. Fraser, C., and Grubbs, R.H. (1995). Synthesis of glycopolymers of controlled molecular weight by ring-opening metathesis polymerization using well-defined functional group tolerant ruthenium carbene catalysts. Macromolecules *28*, 7248–7255.
40. Dias, E.L., Nguten, S.T., and Grubbs, R.H. (1997). Well-defined ruthenium olefin metathesis catalysts: mechanism and activity. J. Am. Chem. Soc. *119*, 3887–3897.
41. Lynn, D.M., Kanaoka, S., and Grubbs, R.H. (1996). Living ring-opening metathesis polymerization in aqueous media catalyzed by well-defined ruthenium carbene complexes. J. Am. Chem. Soc. *118*, 784–790.
42. Khan, M.I., Mandal, D.K., and Brewer, C.F. (1991). Interactions of concanavalin A with glycoproteins. A quantitative precipitation study of concanavalin A with the soybean agglutinin. Carbohydr. Res. *213*, 69–77.
43. Ballerstadt, R., and Schultz, J.S. (1997). Competitive-binding assay method based on fluorescence quenching of ligand held in close proximity by a multivalent receptor. Anal. Chim. Acta *345*, 203–212.
44. Matko, J., and Edidin, M. (1997). Energy transfer methods for detecting molecular clusters on cell surfaces. Methods Enzymol. *278*, 444–462.
45. Lee, Y.C., and Lee, R.T. (1995). Carbohydrate-protein interactions: basis of glycobiology. Acc. Chem. Res. *28*, 321–327.
46. Roy, R. (1996). Synthesis and some applications of chemically defined multivalent glycoconjugates. Curr. Opin. Struct. Biol. *6*, 692–702.
47. Kiessling, L.L., Gestwicki, J.E., and Strong, L.E. (2000). Synthetic multivalent ligands in the exploration of cell surface interactions. Curr. Opin. Chem. Biol. *4*, 696–703.
48. Bertozzi, C.R., and Kiessling, L.L. (2001). Chemical glycobiology. Science *291*, 2357–2364.
49. Ferguson, D.M., and Kollman, P.A. (1991). Can the Leonard-Jones 6–12 function replace the 10–12 form in molecular mechanics calculations. J. Comput. Chem. *12*, 620–626.
50. Naismith, J.H., and Field, R.A. (1996). Structural basis of trimannoside recognition by concanavalin A. J. Biol. Chem. *271*, 972–976.
51. Kraulis, P.J. (1991). Molscript: a program to produce both detailed and schematic plots of protein structures. J. Appl. Crystallogr. *24*, 946–950.
52. Bacon, D., and Anderson, W.F. (1988). A fast algorithm for rendering space-filling molecule pictures. J. Mol. Graph. *6*, 219–220.
53. Darmani, H., and Coakley, W.T. (1991). Contact patterns in concanavalin A agglutinated erythrocytes. Cell Biophys. *18*, 1–13.